Astronomy & Astrophysics

The X-ray afterglows of gamma-ray bursts GRB 001025A and GRB 010220 observed with *XMM-Newton*

D. Watson[1], J. N. Reeves[1], J. Osborne[1], P. T. O'Brien[1], K. A. Pounds[1], J. A. Tedds[1], M. Santos-Lleó[2], and M. Ehle[2]

[1] X-ray Astronomy Group, Dept. of Physics and Astronomy, University of Leicester, Leicester LE1 7RH, UK

[2] XMM-Newton Operations Centre, European Space Agency, Vilspa, Apartado 50727, 28080 Madrid, Spain

Abstract. The X-ray afterglows of GRB 001025A and GRB 010220 were detected by *XMM-Newton* with an average 0.2–10.0 keV flux of 4.4 and 3.3×10^{-14} erg cm^{-2} s^{-1} respectively; the afterglow of GRB 001025A is observed to decay. Afterglows at other wavelengths were not detected for either burst. A set of broadened soft X-ray emission lines are detected in the afterglow of GRB 001025A, at $5.0\,\sigma$ significance above a Galactic-absorbed power-law continuum. The spectra of both afterglows are significantly better fit by a variable abundance thermal plasma model than by an absorbed power-law and are consistent with the observations of GRB 011211, indicating that thermal emission from light elements may be common in the early X-ray afterglows of GRBs.

Key words. gamma rays: bursts – supernovae: general – X-rays: general

1. Introduction

Much of the recent progress in the understanding of gamma-ray bursts (GRBs) has come from bursts detected with good spatial accuracy with *BeppoSAX* and it is particularly at X-ray wavelengths that GRB afterglows are detected (Piro 2001), about half producing no detectable optical afterglow emission (Fynbo et al. 2001). It is also only at X-ray wavelengths that emission lines are detected in afterglows, allowing firm estimates to be made of the cosmological redshifts and the outflow velocities of the afterglow material (Piro et al. 2000; Reeves et al. 2002). *XMM-Newton* (Jansen et al. 2001), with its large effective area, is particularly suited to this work. Previous detections of emission lines in GRB afterglows with *BeppoSAX* and *Chandra* have concentrated on emission from highly-ionised iron (Piro et al. 1998, 2000; Antonelli et al. 2000; Yoshida et al. 2001); however recent observations with *XMM-Newton* have revealed several emission lines at lower energies (Reeves et al. 2002).

Most plausible mechanisms for the production of a GRB involve a newly-formed black hole surrounded by a short-lived accretion disk regardless of the progenitor (Paczynski 1998; MacFadyen & Woosley 1999; Ruffert & Janka 1999; Mészáros 2001). Recent evidence suggests that the progenitors of long-duration GRBs are massive stars (Paczynski 1998; Bloom et al. 1999; MacFadyen & Woosley 1999; Reeves et al. 2002).

Various models have been proposed to account for the emission spectra (in particular the claim of a high equivalent width Fe emission line (Antonelli et al. 2000)) and lightcurves of the afterglow. For instance, the nearby reprocessor model (Rees & Mészáros 2000; Ballantyne & Ramirez-Ruiz 2001;

Kallman et al. 2001) involving reflection of synchrotron emission from the walls of a cone tunnelled out of a massive star, yielding large equivalent width Fe emission lines; or a "supranova" model (Vietri & Stella 1998) which invokes a time delay (≳30 days) between an initial supernova (SN) explosion and the GRB, giving a spectrum briefly dominated either by the recombination of Fe in a photoionised plasma (Vietri & Stella 1998) or reflection of synchrotron emission off the walls of a wide funnel excavated in the SN remnant (Vietri et al. 2001). Recently, Reeves et al. (2002) have suggested that the early X-ray afterglow spectrum of GRB 011211 is dominated by thermal emission from a metal-enriched, but notably Fe-poor collisionally-ionised plasma ejected in a recent SN explosion and heated by the GRB.

In Sect. 2 we report on observations of two GRB afterglows with *XMM-Newton*, presenting the spectra in Sect. 3. In Sect. 4 these results are discussed and their implications for other X-ray observations of afterglows examined. Our conclusions are in Sect. 5. Unless otherwise stated, all errors quoted are 90% confidence limits for one parameter of interest. A cosmology where $H_0 = 75$ km s^{-1} Mpc^{-1} and $q_0 = 0.5$ is assumed throughout.

2. Observations and data reduction

2.1. GRB 001025A

Smith et al. (2000) and Hurley et al. (2000) report detection of a GRB by the RXTE all-sky monitor, NEAR and *Ulysses* beginning at 03:10:05 UT on 25 October 2000. It had a duration of ~5 s, a fluence of 3.2×10^{-6} erg cm^{-2} and a peak

flux of 2.0×10^{-6} erg cm^{-2} s^{-1} in the 25–100 keV band as detected by *Ulysses*. No variable source optical counterpart was detected down to an *R*-band magnitude limit of ~24.5 (Fynbo et al. 2000).

XMM-Newton began observing the error-box of GRB 001025A 45 hours after the burst for two EPIC-pn exposures of 8 ks and 16 ks and single 37 ks exposures of the MOS cameras in full frame mode. The thin filters were used in each case.

The data were processed and reduced with the SAS, version 5.2, datasets from both EPIC-MOS cameras were co-added and both EPIC-pn exposures were also co-added and the resulting two datasets fit simultaneously. Source extraction regions were 35″ in radius and an off-source background extraction region of 70″ radius was chosen. Both single and double pattern (as well as triple and quadruple pattern for the MOS), good (FLAG = 0) events were used with the ready-made response matrices[1] provided by the *XMM-Newton* SOC. The spectra were binned with a minimum of 20 counts per bin. The final X-ray source positions were determined after cross-correlation with the USNO A2.0 optical catalogue based on the SAS task *eposcorr* (see Tedds & Watson 2002).

Two sources were detected in the IPN error-box (Altieri et al. 2000a,b); the brighter, with coordinates (J2000) RA 08h36m35.86s, Dec −13°04′12.28″, and a 68% error radius of 0.6″, was seen to decay slowly (at 99.8% confidence), a power-law decay ($F \propto t^{-\beta}$) with index $\beta = 3.0 \pm 1.9$ fitting the lightcurve well. We identify this source as the afterglow of GRB 001025A. The Galactic hydrogen absorbing column in this direction is 6.1×10^{20} cm^{-2} (using the FTOOL *nh*, Dickey & Lockman 1990). Its mean 0.2–10.0 keV flux was 4.4×10^{-14} erg cm^{-2} s^{-1}, corresponding to an afterglow luminosity of 2.8×10^{43} erg s^{-1} using the redshift ($z = 0.53$) determined from the thermal plasma model fit to the data (see Sect. 3.1). The second source is fainter (1.2×10^{-14} erg cm^{-2} s^{-1}) and shows no evidence for variability.

2.2. GRB 010220

GRB 010220 was detected by *BeppoSAX* at 22:51:07 UT on 20 February 2001 and subsequently localised to within a 4′ radius circle; the burst duration was ~40 s, with ~660 count s^{-1} peak flux in the 40–700 keV band (Manzo et al. 2001). No optical counterpart was detected to a limiting magnitude of $R \simeq 23.5$ (Berger et al. 2001), however the burst position is in the Galactic plane ($b^{II} = 1.41$), where the Galactic nebula IC 1805 lies along the line of sight (Castro-Tirado et al. 2001). The Galactic hydrogen absorbing column is 8.6×10^{21} cm^{-2} (using the FTOOL *nh*, Dickey & Lockman 1990). At 14.8 hours after the burst, *XMM-Newton* began observing at the coordinates of the *BeppoSAX* error-circle. The observation of GRB 010220 was contaminated by a high and variable background. To mitigate this effect, only data where the background rate was relatively low were used. The EPIC-pn exposure was 43 ks; screening for flares left 20 ks of good data. Full frame mode

and the medium filter were used for the observation. No data were available from the EPIC-MOS cameras.

The data were processed and reduced with the SAS version 5.2. A source extraction region of 20″ radius and an off-source background extraction region of 80″ radius were chosen. Both single and double pattern, good (FLAG = 0) events were used with the ready-made response matrix[1] provided by the *XMM-Newton* SOC. The spectra were binned with a minimum of twenty counts per bin. Source positions were determined as noted above.

Four sources were detected in the *BeppoSAX* error circle; the brightest source is 18″ from the centre, with the others at >3′. No variability is detected in any of the sources at greater than 2σ confidence. We assume that the brightest source, at coordinates (J2000): RA 02h37m01.66s, Dec +61°45′56.01″ with a 68% confidence error circle of 1.2″ radius is the GRB afterglow. This source decays at 94% confidence, with a best-fit decay index, $\beta = 1.2 \pm 1.0$. Its mean 0.2–10.0 keV flux was 3.3×10^{-14} erg cm^{-2} s^{-1} (corresponding to an afterglow luminosity of 7.3×10^{43} erg s^{-1} in the rest frame 0.2–10.0 keV band based on the best-fit redshift ($z = 1.0$) from the thermal plasma fit to the data).

3. Spectral fitting

In order to test the wider applicability of the collisionally-ionised plasma model proposed by Reeves et al. (2002) to explain the *XMM-Newton* observations of the afterglow of GRB 011211, our new GRB X-ray afterglow data were fit with the same set of models. They were **a)** a power-law, **b)** a power-law with a variable, cold, redshifted absorber, **c)** a variable abundance collisionally-ionised plasma model (the MEKAL model, Mewe et al. 1985; Liedahl et al. 1995) with the abundances of Mg, Si, S, Ar and Ca fit jointly, Ni allowed to vary freely and all other elements fixed at the solar value and **d)** an ionised reflection model (Ballantyne & Ramirez-Ruiz 2001) where the emission arises purely from the X-ray flux scattered off material with twice the solar elemental abundance, also modified by a cold, redshifted absorber. In all cases an absorber fixed at the Galactic value was included.

In order to test the significance of the fit improvements, 10 000 spectra were simulated using the parameters derived from fitting an absorbed power-law (model **b**) to the data in each case. Models **b)** and **c)** were fit to the simulated data and the difference in χ^2 computed. The results of these tests are reported in Table 1. Using a random gaussian distribution of initial parameters centred on the parameters derived from fitting an absorbed power-law to the data, a second set of 10 000 simulated spectra was generated. This second set of simulations yielded results consistent with the first.

3.1. GRB 001025A

The spectrum for this afterglow is significantly better fit by the thermal plasma model than the absorbed power-law (Table 1) – only 13 in 10 000 simulations are as good a fit. While the continuum shape dictates that the plasma temperatures in the simulated spectra will be consistent with each other and with the fit

---

[1] http://xmm.vilspa.esa.es/ccf/epic

Table 1. χ^2/degrees of freedom for model fits to both GRB afterglows. Model **a)** is a power-law. Model **b)**, is the same as model **a)** modified by a cold, redshifted absorber. **c)** is a variable abundance collisionally ionised plasma model with the abundances of Mg, Si, S, Ar and Ca fit jointly, Ni allowed to vary freely and all other elements fixed at the solar value. Model **d)** is an ionised reflection model where the emission arises purely from the X-ray flux scattered off material with twice the solar elemental abundance, also modified by a cold, redshifted absorber. In all cases an absorber fixed at the Galactic value was included. Column four is the percentage of spectral fits (simulated using model **b)**) with greater χ^2 differences between models **b)** and **c)** than the real data.

GRB	a	b	MC Prob.	c	d
001025A	95.7/66	68.6/64	0.13%	54.1/63	65.5/63
010220	15.4/15	14.8/14	0.16%	5.2/13	6.7/12

Table 2. Best-fit parameters from spectral fits to the afterglow data. In the upper section, parameters of the fit to the collisionally ionised plasma model (model **c** in Sect. 3) are presented. Parameters of the best fit to an absorbed power-law (model **b**) are included for reference in the lower section. Values in parentheses are 90% confidence limits for one interesting parameter.

GRB	T (keV)	z	Mg/Si/S/Ar/Ca (Solar Abundances)	Ni
001025A	3.4 (2.9–3.9)	0.53 (0.50–0.55)	2.0 (0.7–3.7)	26 (14–40)
010220	6.0 (3.6–12.7)	1.0 (0.97–1.07)	10 frozen	95 (32–248)

	Γ	z	$N_{\rm H}$ (10^{21} cm^{-2})
001025A	2.50 (2.26–2.97)	0.5 (0–7.1)	3 (1–184)
010220	2.1 (1.5–3.1)	1.0 frozen	16 (0–67)

to the real data, only four of the redshifts determined from the thirteen best-fit simulated spectra are within 90% confidence limits of the value from the real data, reinforcing the fact that the emission lines are not systematic deviations.

The need for the thermal emission component arises from the soft excess observed between ~0.5 and 2 keV (Fig. 1), which we suggest may be due to the blend of lines from Mg, Si, S, Ar and Ni-L. The thermal plasma model fit to the data yields a temperature of 3.4 keV and a redshift of 0.53 and does not require super-solar abundance of light metals (Table 2).

In order to parameterise the line emission, a power-law with Galactic absorption and Gaussian emission lines was fit to the data, allowing the line widths to vary together. For five emission lines, the χ^2 is 40.1 for 55 degrees of freedom, (giving a null hypothesis probability of 3×10^{-4} ($3.6\,\sigma$) over the absorbed power-law and 5×10^{-7} ($5.0\,\sigma$) over a power-law with Galactic absorption. Adding lines to a bremsstrahlung continuum yielded similar significances, (3×10^{-4} ($3.6\,\sigma$) over the absorbed bremsstrahlung and 2×10^{-4} ($3.8\,\sigma$) over

a bremsstrahlung with Galactic absorption), though the fit was worse, $\chi^2 = 45.4$ for 55 degrees of freedom.

The best-fit energies for the lines are: $4.7^{+0.8}_{-0.4}$, 2.2 ± 0.1, 1.64 ± 0.07, 1.16 ± 0.05 and $0.80^{+0.04}_{-0.05}$ keV with a *FWHM* of 240^{+70}_{-60} eV with individual line significances (null hypothesis probabilities) of 0.12, 0.02, 8×10^{-4}, 8×10^{-4} and 4×10^{-4} respectively. Single line significances were determined by using the best-fit Galactic-absorbed power-law with five Gaussian emission lines and removing individual lines to assess their f-statistic. Probabilities were then determined using the f-test. The observed equivalent width is ~800 eV for the 4.7 keV line and ~400 eV for the others. Fitting the Kα emission lines of Mg xii (1.46 keV), Si xiv (1.99 keV), S xvi (2.60 keV), Ar xviii (3.30 keV) and ^{56}Ni xxviii (8.10 keV), gives a best-fit redshift of $0.7^{+0.3}_{-0.1}$. This redshift is within two standard deviations of the redshift determined from the thermal plasma fit (Table 2). Allowing for an outflow velocity of $0.0-0.1\,c$ (Reeves et al. 2002), we conclude that the redshift of the host galaxy is likely to lie in the range 0.5–1.2.

It has been suggested that reflection of synchrotron emission from ionised material could produce the emission lines observed in GRB afterglows (e.g., Ballantyne et al. 2002). An ionised reflection model is as good a fit to the data as an absorbed power-law; however, adding a power-law continuum to the reflection component disimproves the fit significantly, indicating that the afterglow must be viewed so that little of the continuum is observed, if this fit is to be acceptable. This implies a line-of-sight outside the GRB cone, a possibility ruled out by the detection of the GRB in the first place. In any case, the ionised pure reflection model does not fit the soft excess as well as the thermal plasma model (Table 1). Modifications to the reflection model (such as including contributions from S, Ar and Ca) could improve the fit to the data.

3.2. GRB 010220

A power-law model with Galactic absorption is an acceptable fit to the data, however the single clearest deviation in the spectrum of GRB 010220 (Fig. 2) is the feature near 3.9 keV; adding an unresolved Gaussian line (equivalent width = $1.8^{+0.8}_{-1.2}$ keV) to the power-law fit improves the fit at >99% significance ($\chi^2 = 7.5$ for 13 degrees of freedom) and is the only emission feature in the spectrum. While the relatively poor statistics do not enable us to detect individual emission lines at lower energies (e.g. Si or S Kα), the thermal plasma model is significantly preferred to the absorbed power-law model with a null hypothesis probability of 0.0016 using statistics from the Monte Carlo simulations. Allowing the abundance of Fe to vary did not significantly improve the thermal plasma fit as the energy of the Fe Kα emission is too low relative to the emission at low energies and is not broad enough to fit the excess alone. The best-fit Fe abundance is consistent with solar abundance; allowing Ni to vary improves the fit at >99% confidence as it fits most of the 3.9 keV emission feature.

The pure ionised reflection model in this case is a better fit than the absorbed power-law model (Table 1) primarily due to fitting Fe emission (at lower redshift than the thermal plasma
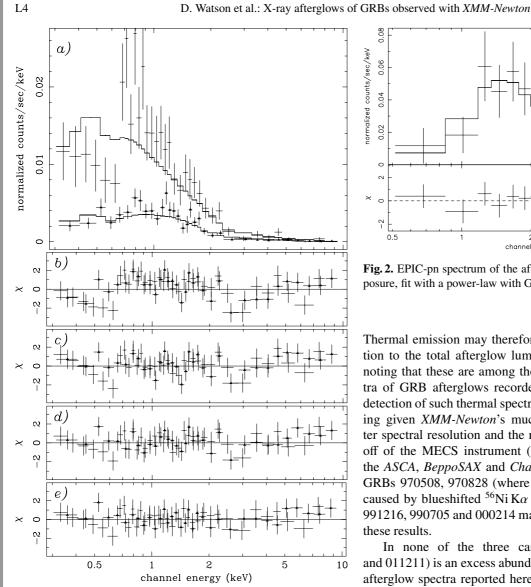
Fig. 1. EPIC-pn (crosses) and combined MOS (filled triangles) spectrum of the afterglow of GRB 001025A; **a)** data fit to a Galactic-absorbed power-law model; **b)** residuals to plot **a)**; **c)** fit residuals to a Galactic-absorbed power-law model with variable redshifted absorption; **d)** fit residuals to a collisionally-ionised plasma model with variable abundance of Mg, Si, S, Ar and Ca and freely variable Ni abundance (VMEKAL), absorbed by the Galactic column; **e)** fit residuals to a Galactic-absorbed power-law and five Gaussian emission lines model, allowing the line widths to vary jointly.

model) to the ~3.9 keV feature, however the addition of any power-law continuum disimproves the fit as for GRB 001025A.

4. Discussion

It is clear that for the X-ray afterglows of GRBs 001025A and 010220, the type of collisionally-ionised plasma model fit to the afterglow of GRB 011211 (Reeves et al. 2002) is a better fit to the data than an absorbed power-law. The detection of a thermal spectrum in three GRB afterglows with *XMM-Newton* indicates that this behaviour is relatively common hours to days after the burst among the long duration GRBs.
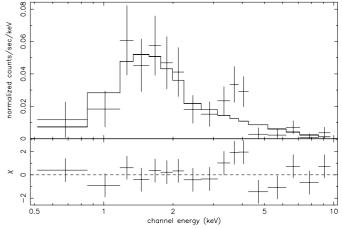

Fig. 2. EPIC-pn spectrum of the afterglow of GRB 010220, 20 ks exposure, fit with a power-law with Galactic absorption.

Thermal emission may therefore make a significant contribution to the total afterglow luminosity of a GRB. It is worth noting that these are among the best quality soft X-ray spectra of GRB afterglows recorded to date and the absence of detection of such thermal spectra with *BeppoSAX* is not suprising given *XMM-Newton*'s much greater sensitivity and better spectral resolution and the relatively high low-energy cut-off of the MECS instrument (~2 keV). A re-examination of the *ASCA*, *BeppoSAX* and *Chandra* data of the afterglows of GRBs 970508, 970828 (where the 5.04 keV feature could be caused by blueshifted ^{56}Ni Kα emission blueshifted by 0.2c), 991216, 990705 and 000214 may be worthwhile in the light of these results.

In none of the three cases (GRBs 001025A, 010220 and 011211) is an excess abundance of Fe required and in both afterglow spectra reported here a large over-abundance of Ni (or possibly Co) is required, consistent with the idea that the SN–GRB lag must be of the order of days, not months, though it is worth noting that this timescale can be extended where the material is ionised (McLaughlin & Wijers 2002).

Using the model proposed by Reeves et al. (2002) to explain the observations of GRB 011211 it is difficult to place precise limits on the size of the SN shell, the expansion speed and the time delay between the burst and the initial SN from the spectra of these afterglows as the redshifts of the host galaxies are unknown and the redshifts derived from the X-ray spectra are not as tightly constrained as in GRB 011211. It is possible however, to constrain the minimum radius of the SN ejecta shell and its mass on the assumption that the duration of the thermal emission is due primarily to light-crossing time over the illuminated shell. With no collimation of the GRB and where the thermal emission lasts at least as long as the time between the burst and the afterglow observation (~7 and 30 hours), the minimum shell radii are 8×10^{14} cm and 3×10^{15} cm corresponding to SN-GRB delays of at least 3 and 12 days for GRB 010220 and GRB 001025A respectively and illuminated shell masses of 0.9 and 1.1 $M_\odot$ using the best fit emission measure, temperature and redshifts from the MEKAL model. Reeves et al. (2002) calculate a delay of a few days and

at most two weeks between the SN and the GRB, consistent with these results, though the SN-GRB time delay distribution has so far not been defined. The time delay for GRB 001025A is suggestive since the half-life of the most abundant product of Si burning, ^{56}Ni, is 6.1 days decaying primarily to ^{56}Co with a half-life of 77.3 days to ^{56}Fe (although see, on half-lives of ionised species, McLaughlin & Wijers 2002). In this scenario, much of the emission observed near 1 keV in the spectrum of GRB 001025A could then be due to L-shell emission from ^{56}Co. The spectrum however is not sufficiently good to investigate this possibility.

Recent analysis of the *XMM-Newton* spectrum of GRB 020322, with a signal to noise ratio comparable to the X-ray spectrum of GRB 011211, shows no evidence of emission features (Watson et al. in prep.) 15 hours after the burst; evidence that if thermal emission occurs in every afterglow, it may be relatively short-lived.

The prospect that thermal emission may contribute significantly to the X-ray luminosity of afterglows could resolve the problem of bursts with apparently high X-ray column densities but low optical extinctions, 10–100 times smaller than expected (Galama & Wijers 2001). The curvature of low-quality thermal X-ray spectra can be approximated by an absorbed power-law, giving much larger absorbing columns than are required by the thermal spectra.

Another implication of the data reported here is that GRBs without significant optical emission, "dark GRBs" (Reichart & Yost 2001; Djorgovski et al. 2001), may not always need to have significant extinction (Taylor et al. 2000; Reichart & Yost 2001; Piro et al. 2002), be intrinsically different (Lazzati et al. 2002) or be very distant (Lamb & Reichart 2000). A soft X-ray spectrum dominated by thermal emission will lead to an overestimation of the expected optical flux where this is predicted assuming a synchrotron-dominated X-ray flux below 10 keV (Djorgovski et al. 2001).

5. Conclusions

XMM-Newton detected the afterglows of GRB 001025A and GRB 010220 the former showing a decaying lightcurve. Positions accurate to ∼1″ were determined; this makes it feasible for optical spectroscopy to be used to confirm the X-ray redshift reported in this paper for the host galaxies of these GRBs, in particular for the host of GRB 001025A, where the extinction is relatively low. In both cases, the X-ray spectra are significantly better fit by the thermal plasma model proposed by Reeves et al. (2002) to explain the line features in GRB 011211 than by an absorbed power-law and in the case of GRB 001025A the thermal plasma model is a significantly better fit than an ionised reflection model. The parameters determined from these thermal fits are consistent with their suggested scenario. It seems likely that a large contribution from highly-ionised light metals is a common feature in the X-ray spectra of GRB afterglows hours to days after the burst and the detection of thermal emission in three of the four *XMM-Newton*–detected afterglows implies that this may be a significant component in the total afterglow luminosity of all long GRBs.

References

Altieri, B., Schartel, N., Lumb, D., Piro, L., & Parmar, A. 2000a, GRB Coordinates Network Circular, 884

Altieri, B., Schartel, N., Santos, M., et al. 2000b, GRB Coordinates Network Circular, 869

Antonelli, L. A., Piro, L., Vietri, M., et al. 2000, ApJ, 545, L39

Ballantyne, D. R., & Ramirez-Ruiz, E. 2001, ApJ, 559, L83

Ballantyne, D. R., Ramirez-Ruiz, E., Lazzati, D., & Piro, L. 2002 [astro-ph/0206116]

Berger, E., Frail, D. A., Price, P. A., et al. 2001, GRB Coordinates Network Circular, 958, 1

Bloom, J. S., Kulkarni, S. R., Djorgovski, S. G., et al. 1999, Nature, 401, 453

Castro-Tirado, A., Castro Cerón, J. M., Mateo Sanguino, T. J., et al. 2001, GRB Coordinates Network Circular, 957, 1

Dickey, J. M., & Lockman, F. J. 1990, ARA&A, 28, 215

Djorgovski, S. G., Frail, D. A., Kulkarni, S. R., et al. 2001, ApJ, 562, 654

Fynbo, J. P. U., Moller, P., Milvang-Jensen, B., et al. 2000, GRB Coordinates Network Circular, 867

Fynbo, J. U., Jensen, B. L., Gorosabel, J., et al. 2001, A&A, 369, 373

Galama, T. J., & Wijers, R. A. M. J. 2001, ApJ, 549, L209

Hurley, K., Cline, T., & Smith, D. 2000, GRB Coordinates Network Circular, 863

Jansen, F., Lumb, D., Altieri, B., et al. 2001, A&A, 365, L1

Kallman, T. R., Meszaros, P., & Rees, M. J. 2001 [astro-ph/0110654]

Lamb, D. Q., & Reichart, D. E. 2000, ApJ, 536, 1

Lazzati, D., Covino, S., & Ghisellini, G. 2002, MNRAS, 330, 583

Liedahl, D. A., Osterheld, A. L., & Goldstein, W. H. 1995, ApJ, 438, L115

Mészáros, P. 2001, Science, 291, 79

MacFadyen, A. I., & Woosley, S. E. 1999, ApJ, 524, 262

Manzo, R., Kaptein, R. G., in't Zand, J. J. M., et al. 2001, GRB Coordinates Network Circular, 956

McLaughlin, G. C., & Wijers, R. A. M. J. 2002 [astro-ph/0205321]

Mewe, R., Gronenschild, E. H. B. M., & van den Oord, G. H. J. 1985, A&AS, 62, 197

Paczynski, B. 1998, ApJ, 494, L45

Piro, L. 2001, in Gamma-Ray Bursts in the Afterglow Era, ed. E. Costa, F. Frontera, & J. Hjorth (Springer), 97

Piro, L., Amati, L., Antonelli, L. A., et al. 1998, A&A, 331, L41

Piro, L., Frail, D. A., Gorosabel, J., et al. 2002 [astro-ph/0201282]

Piro, L., Garmire, G., Garcia, M., et al. 2000, Science, 290, 955

Rees, M. J., & Mészáros, P. 2000, ApJ, 545, L73

Reeves, J. N., Watson, D., Osborne, J. P., et al. 2002, Nature, 416, 512

Reichart, D. E., & Yost, S. A. 2001 [astro-ph/0107545]

Ruffert, M., & Janka, H.-T. 1999, A&A, 344, 573

Smith, D. A., Levine, A. M., Remillard, R., Hurley, K., & Cline, T. 2000, GRB Coordinates Network Circular, 861

Taylor, G. B., Bloom, J. S., Frail, D. A., et al. 2000, ApJ, 537, L17

Tedds, J. A., & Watson, M. G. 2002, in New Visions of the X-Ray Universe in the XMM-Newton and Chandra Era, ed. F. Jansen, ESA SP-488

Vietri, M., Ghisellini, G., Lazzati, D., Fiore, F., & Stella, L. 2001, ApJ, 550, L43

Vietri, M., & Stella, L. 1998, ApJ, 507, L45

Yoshida, A., Namiki, M., Yonetoku, D., et al. 2001, ApJ, 557, L27

Letter to the Editor